01 Jan 1984

Dipole Moment And Potential Energy Functions Of The X ¹Σ + And A 1Σ+ States Of NaH

W. T. Zemke

Ronald E. Olson
Missouri University of Science and Technology, olson@mst.edu

K. K. Verma

W. C. Stwalley

et. al. For a complete list of authors, see https://scholarsmine.mst.edu/phys_facwork/2530

Recommended Citation

W. T. Zemke et al., "Dipole Moment And Potential Energy Functions Of The X ¹Σ + And A 1Σ+ States Of NaH," *The Journal of Chemical Physics*, vol. 80, no. 1, pp. 356 - 364, American Institute of Physics, Jan 1984.
The definitive version is available at https://doi.org/10.1063/1.446455

RESEARCH ARTICLE | JANUARY 01 1984

Dipole moment and potential energy functions of the $X\ ^1\Sigma^+$ and $A\ ^1\Sigma^+$ states of NaH

W. T. Zemke; R. E. Olson; K. K. Verma; W. C. Stwalley; B. Liu

J. Chem. Phys. 80, 356–364 (1984)
https://doi.org/10.1063/1.446455

Dipole moment and potential energy functions of the $X\,^1\Sigma^+$ and $A\,^1\Sigma^+$ states of NaH

W. T. Zemke
Department of Chemistry, Wartburg College, Waverly, Iowa 50677

R. E. Olson
Department of Physics, University of Missouri, Rolla, Missouri 65401

K. K. Verma[a] and W. C. Stwalley
Iowa Laser Facility and Departments of Chemistry and Physics, University of Iowa, Iowa City, Iowa 52242

B. Liu
IBM Research Laboratory, San Jose, California 95193

(Received 12 August 1983; accepted 12 September 1983)

Calculated radiative transition probabilities between all vibrational levels in the $X\,^1\Sigma^+$ state ($v = 0$–21) and in the $A\,^1\Sigma^+$ state ($v = 0$–32) of NaH are given. In addition, the calculated spontaneous emission lifetimes for vibrational–rotational levels ($J = 0,1$) and the calculated dipole moments for these same levels are given. The calculations use new hybrid potential energy curves based on Rydberg–Klein–Rees (RKR) and *ab initio* potential curves. The RKR curve for the X state is new. The calculations use new *ab initio* dipole moment functions of internuclear distance.

I. INTRODUCTION

This paper on NaH is part of a larger study (e.g., Yang and Stwalley,[1] Stwalley and Yang[2]) on the spectroscopy and structure of ground and excited states of the alkali metal hydrides. The study has included both experimental and theoretical results; for example, an earlier paper[3] on the $A\,^1\Sigma^+$ state of LiH demonstrates the beneficial interaction between experiment and theory in the determination of a high quality dipole moment function.

This study on NaH includes an analysis of several theoretical dipole moment functions and experimental RKR potential energy curves. We present a new RKR potential curve for the $X\,^1\Sigma^+$ state and new hybrid potential curves and dipole moment functions for both $X\,^1\Sigma^+$ and $A\,^1\Sigma^+$ states for all internuclear distances R. Finally, we present radiative transition probabilities, lifetimes, and dipole moments of all vibrational levels within both states.

In Sec. II we discuss construction of the potential energy functions $V(R)$. In Sec. III we discuss construction of the dipole moment functions $\mu(R)$. Results and discussion of the transition probabilities, lifetime, and dipole moment calculations are presented in Sec. IV; comparisons with other theoretical and experimental results are given. In Sec. V we summarize our results.

II. POTENTIAL FUNCTIONS

A. $X\,^1\Sigma^+$ state of NaH

The hybrid potential energy curve for the $X\,^1\Sigma^+$ state (Fig. 1 and Tables I and II) is constructed throughout the well in a fashion similar to that[4] for the X state of LiH. The full potential consists of a spline fit of the $V(R)$ points over the dominant region ($2.550\,802 \leqslant R \leqslant 17.0a_0$; see Table II) plus an exponential function for $R \leqslant 2.550\,802a_0$ and a long range $-C_n/R^n$ expansion for $R \geqslant 17.0a_0$ (see Table I).

The region about R_e is from a new RKR calculation with $0 \leqslant v \leqslant 11$. A dissociation energy $D_e = 15\,900\ \mathrm{cm}^{-1}$ is assumed.[1] The long range region of the potential $V_{LR}(R)$ is well defined:

$$V_{LR}(R) = -C_6/R^6 - C_8/R^8 - C_{10}/R^{10},$$

where the C_6, C_8, and C_{10} coefficients are directly from Proctor and Stwalley.[5] The LeRoy criterion[6,7] for the onset of breakdown of the $-C_n/R^n$ expansion occurs at $\sim 14a_0$, so we take $V_{LR}(R)$ for $R \geqslant 17.0a_0$.

The Olson and Liu[9] *ab initio* $V(R)$ points from 7.0 to $15.0a_0$ are scaled to smoothly fit onto the RKR curve near the outermost turning point R_{11+} and onto the long range potential at $R = 17a_0$. The inner wall of the curve consists of an exponential function of the form $Ae^{-BR} - C$ and is based on the Olson–Liu $V(R)$ points at 1.75, 2.00, and $2.50a_0$ and shifted to fit smoothly onto the innermost RKR turning point $R_{11-} = 2.550\,802a_0$.

Previous RKR curves include those of Orth *et al.*[10] ($0 \leqslant v \leqslant 8$) and Giroud and Nedelec[11] ($0 \leqslant v \leqslant 15$). Unfortunately, the Giroud–Nedelec values are reported only to 0.001 Å. Our new turning points agree to within 0.0005 Å with those of Orth *et al.*,[10] but both sets disagree with the Giroud–Nedelec turning points (especially 0.007 Å for R_{0-} and 0.009 Å for R_{0+}), contrary to their[11] "note added in proof" statement. Sastry *et al.*[12] have also determined spectroscopic constants for the $X\,^1\Sigma^+$ state; but they report only rotational (microwave) constants that do not permit the construction of an RKR curve.

The RKR curve presented in Table II is constructed

[a] Present address: 3B-611A, Bell Telephone Laboratory, Holmdel, New Jersey 07733.

 0021-9606/84/010356-09$02.10

TABLE I. Potential energy curves (in a.u. with respect to the dissociation limit) for $X\,^1\Sigma^+$ and $A\,^1\Sigma^+$ states of NaH. $V(R)$ and dV/dR are continuous.

State	Region	Range of R (a_0)	Function
$X\,^1\Sigma^+$	I	$R<2.550\,802$	$(16.5689)\,e^{-2.275\,33\,R} - 0.072\,172\,8$
	II	$2.550\,802<R<17.0$	Tensioned cubic spline fit to the points in Table II
	III	$17.0<R$	$-73.70/R^6 - 3742/R^8 - 267\,100/R^{10}$
$A\,^1\Sigma^+$	I	$R<3.185\,32$	$(2.593\,37)e^{-1.327\,74\,R} - 0.051\,692\,8$
	II	$3.185\,32<R<20.0$	Tensioned cubic spline fit to the points in Table III
	III	$20.0<R$	$-201.6/R^6 - 38\,462/R^8$

from these new spectroscopic constants (all in cm^{-1}):

$$\omega_e = 1171.750, \quad B_e = 4.903\,19\ (R_e = 1.887\,07\ \text{Å}),$$
$$\omega_e x_e = 19.740\,5, \quad \alpha_e = 0.139\,20,$$
$$\omega_e y_e = 0.192\,25, \quad \gamma_e = 0.001\,899\,3,$$
$$\omega_e z_e = -0.007\,4914, \quad \epsilon_e = -0.000\,106\,76.$$

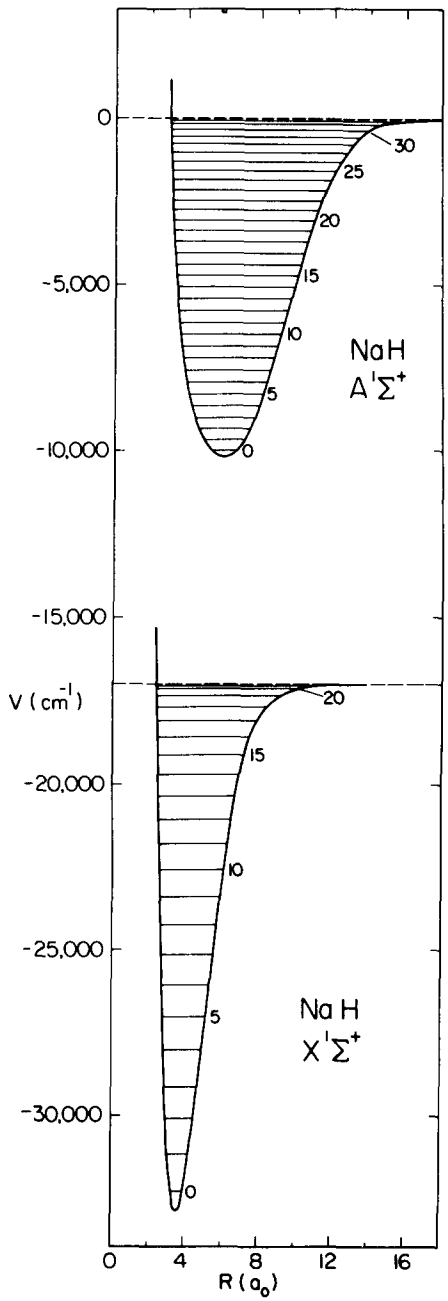

FIG. 1. Vibrational levels of the hybrid $X\,^1\Sigma^+$ ($v = 0$–21) and $A\,^1\Sigma^+$ ($v = 0$–32) potential energy curves in NaH.

These constants were based on a combination of data for $v \leqslant 11$ included in Refs. 10, 11, and 12. Higher v values in Ref. 11 were not included because of the erratic behavior of B_v for these levels.

This RKR curve is better than the earlier one (for $v \leqslant 8$)

TABLE II. Points used in the intermediate region II (see Table I) of the potential for the $X\,^1\Sigma^+$ state of NaH.

R (a_0)[a]	V (a.u.)[a]	Source[b]
2.550 802	− 0.022 205 6	R_{11-}
2.576 990	− 0.025 701 8	R_{10-}
2.606 257	− 0.029 367 9	R_{9-}
2.639 061	− 0.033 201 0	R_{8-}
2.676 012	− 0.037 199 0	R_{7-}
2.717 955	− 0.041 360 6	R_{6-}
2.766 100	− 0.045 685 3	R_{5-}
2.822 284	− 0.050 173 4	R_{4-}
2.889 504	− 0.054 826 1	R_{3-}
2.973 243	− 0.059 645 4	R_{2-}
3.085 685	− 0.064 634 1	R_{1-}
3.269 457	− 0.069 795 8	R_{0-}
3.566 044	− 0.072 445 7	R_e[c]
3.926 517	− 0.069 795 8	R_{0+}
4.239 926	− 0.064 634 1	R_{1+}
4.484 732	− 0.059 645 4	R_{2+}
4.703 898	− 0.054 826 1	R_{3+}
4.910 000	− 0.050 173 4	R_{4+}
5.108 979	− 0.045 685 3	R_{5+}
5.304 375	− 0.041 360 6	R_{6+}
5.498 659	− 0.037 199 0	R_{7+}
5.693 791	− 0.033 201 0	R_{8+}
5.891 502	− 0.029 367 9	R_{9+}
6.093 461	− 0.025 701 8	R_{10+}
6.301 393	− 0.022 205 6	R_{11+}
7.0	− 0.012 420 0	*ab initio*[d]
8.0	− 0.004 728 5	*ab initio*
10.0	− 0.000 598 7	*ab initio*
11.75	− 0.000 111 1	*ab initio*
12.0	− 0.000 088 9	*ab initio*
13.5	− 0.000 027 5	*ab initio*
15.0	− 0.000 011 6	*ab initio*
17.0	− 0.000 003 721	long range[e]

[a] $1a_0 = 0.529\,177$ Å; 1 a.u. = 1 hartree = 219 474.624 cm^{-1} (1 eV = 8065.479 cm^{-1}).

[b] Except for the *ab initio* and long range entries, $V(R_{v\pm}) = [G(v) + Y_{00}] - D_e$, where $G(v)$ is the energy level for vibrational quantum number v and R_{v-} and R_{v+} are the inner and outer RKR turning points for level v. Y_{00} is the Dunham correction to the zero point energy such that $G(0) + Y_{00}$ = Z.P.E. ($Y_{00} = 0.6301\ cm^{-1}$). D_e is the dissociation energy (Ref. 1) with respect to the bottom of the well.

[c] R_e is the equilibrium internuclear distance.

[d] These are theoretical $V(R)$ points from Ref. 9, multiplied by the scaling factor γ_x to shift the theoretical points downwards to fit smoothly onto the RKR points; $\gamma_x = V_{RKR}(6.0a_0)/V_{theo}(6.0a_0) = 1.057\,83$.

[e] $V(R) = V_{LR}(R = 17.0a_0)$ based on the long-range coefficients C_6, C_8, and C_{10}; see Table I.

by Orth *et al.*[10] for the $X\ ^1\Sigma^+$ state because the fit includes levels up to $v = 11$ and new data from Refs. 11 and 12. This curve covers 70% rather than 57% of the bottom of the well (when $v \leqslant 8$).

B. $A\ ^1\Sigma^+$ state of NaH

The hybrid potential energy curve for the $A\ ^1\Sigma^+$ state (Fig. 1 and Tables I and III) is constructed in a fashion similar to that for the $X\ ^1\Sigma^+$ state. The full potential consists of a spline fit of the $V(R)$ points over the dominant region ($3.185\ 32 \leqslant R \leqslant 20.0a_0$; see Table III) plus an exponential for $R \leqslant 3.185\ 32a_0$ and a long range $-C_n/R^n$ expansion for $R \leqslant 20.0a_0$ (see Table I).

The region about R_e is from a prior RKR calculation[10] with $0 \leqslant v \leqslant 20$. A dissociation energy $D_e = 10\ 137\ \text{cm}^{-1}$ is assumed.[1] The long range region of the potential is well defined:

$$V_{LR}(R) = -C_6/R^6 - C_8/R^8,$$

where the C_6 and C_8 coefficients are estimated from those[13] for the $A\ ^1\Sigma^+$ state of LiH. The LeRoy criterion[6,7] for the A state occurs at $\sim 16.3a_0$, so we take the long range $V_{LR}(R)$ form for $R \geqslant 20.0a_0$.

The Olson and Liu[9] *ab initio* points from 11.75 to $15.0a_0$ are scaled to fit smoothly onto the RKR curve near the outermost turning point R_{20+} and onto the long range potential at $R = 20a_0$. The inner wall of the curve is of exponential form and based on the Olson and Liu points at 2.50, 3.00, and $3.25a_0$; it fits smoothly onto the innermost turning point $R_{20-} = 3.185\ 32a_0$.

TABLE III. Points used in the intermediate region II (see Table I) of the potential for the $A\ ^1\Sigma^+$ state of NaH.

$R\ (a_0)$[a]	V(a.u.)[a]	Source[b]
3.185 32	−0.013 925 8	R_{20-}
3.215 37	−0.015 400 6	R_{19-}
3.247 69	−0.016 904 0	R_{18-}
3.282 65	−0.018 431 8	R_{17-}
3.320 25	−0.019 981 0	R_{16-}
3.361 26	−0.021 549 7	R_{15-}
3.405 67	−0.023 136 3	R_{14-}
3.453 67	−0.024 738 9	R_{13-}
3.505 82	−0.026 355 6	R_{12-}
3.562 89	−0.027 984 1	R_{11-}
3.625 63	−0.029 621 3	R_{10-}
3.695 36	−0.031 263 2	R_{9-}
3.773 22	−0.032 905 7	R_{8-}
3.861 85	−0.034 543 4	R_{7-}
3.964 08	−0.036 171 2	R_{6-}
4.084 27	−0.037 783 4	R_{5-}
4.227 51	−0.039 374 8	R_{4-}
4.403 63	−0.040 940 5	R_{3-}
4.626 81	−0.042 477 0	R_{2-}
4.926 52	−0.043 982 4	R_{1-}
5.392 53	−0.045 457 0	R_{0-}
6.034 66	−0.046 187 6	R_e[c]
6.641 26	−0.045 457 0	R_{0+}
7.071 36	−0.043 982 4	R_{1+}
7.372 01	−0.042 477 0	R_{2+}
7.624 29	−0.040 940 5	R_{3+}
7.851 25	−0.039 374 8	R_{4+}
8.063 09	−0.037 783 4	R_{5+}
8.265 29	−0.036 171 2	R_{6+}
8.461 63	−0.034 543 4	R_{7+}
8.654 57	−0.032 905 7	R_{8+}
8.845 44	−0.031 263 2	R_{9+}
9.035 54	−0.029 621 3	R_{10+}
9.225 65	−0.027 984 1	R_{11+}
9.416 13	−0.026 355 6	R_{12+}
9.607 37	−0.024 738 9	R_{13+}
9.799 56	−0.023 136 3	R_{14+}
9.993 07	−0.021 549 7	R_{15+}
10.187 90	−0.019 981 0	R_{16+}
10.384 81	−0.018 431 8	R_{17+}
10.584 93	−0.016 904 0	R_{18+}
10.789 59	−0.015 400 6	R_{19+}
11.001 24	−0.013 925 8	R_{20+}
11.75	−0.009 074 0	*ab initio*[d]
12.0	−0.007 722 0	*ab initio*
13.5	−0.002 367 0	*ab initio*
15.0	−0.000 623 0	*ab initio*
20.0	−0.000 004 652	long range[e]

[a] $1a_0 = 0.529\ 177$ Å; 1 a.u. = 219 474.624 cm^{-1}.
[b] Same description as footnote b in Table II; $Y_{00} = 0.86\ \text{cm}^{-1}$.
[c] R_e is the equilibrium internuclear distance.
[d] These are theoretical $V(R)$ points from Ref. 9, multiplied by the scaling factor γ_A to shift the theoretical points downwards to fit smoothly onto the RKR points of Ref. 10; $\gamma_A = V_{RKR}(10.0a_0)/V_{theo.}(10.0a_0) = 1.043\ 35$.
[e] $V(R) = V_{LR}(R = 20.0a_0)$ based on the long-range coefficients C_6 and C_8; see Table I.

III. DIPOLE MOMENT FUNCTIONS

A. $X\ ^1\Sigma^+$ state of NaH

The dipole moment function $\mu(R)$ is constructed in a fashion similar to that for the potential curve (see Fig. 2 and Tables IV and V). The $\mu(R)$ function consists of three regions, given in Table IV. Region II (from 2.0 to $30.0a_0$) is the physically important region and the most significant region in our calculations; it consists of a spline fit to the points given in Table V. Inside $2.0a_0$ (region I), the potential curve is

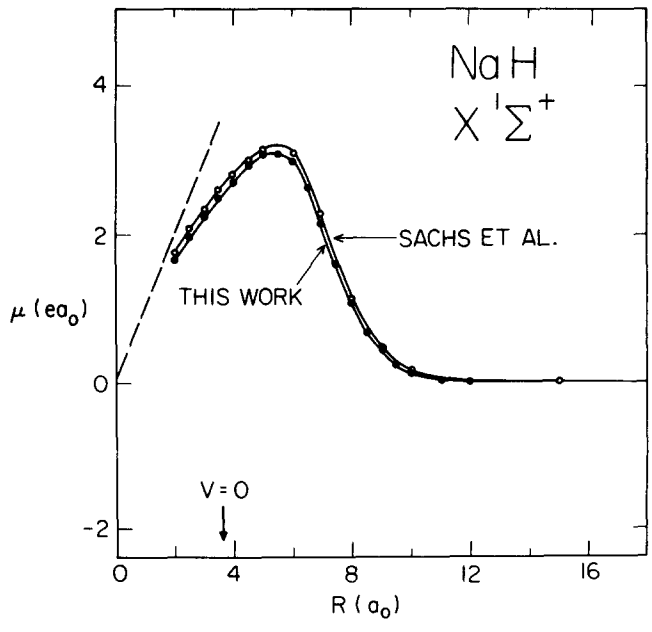

FIG. 2. Dipole moment function $\mu(R)$ (in a.u.) for the $X\ ^1\Sigma^+$ ground state of NaH. The smooth curves through the data are spline fits to the points found in Table V or Sachs *et al.* (Ref. 14). The dashed line at small R is the pure ionic curve for Na^+H^-. The arrow indicates the R location corresponding to the vibrationally averaged dipole moment $\mu_{v=0}(J=0)$.

TABLE IV. The dipole moment functions $\mu(R)$ in atomic units ($e\,a_0$) for the $X\ ^1\Sigma^+$ an $A\ ^1\Sigma^+$ states of NaH.

State	Region	Range of R (a_0)	Function
$X\ ^1\Sigma^+$	I	$R \leqslant 2.0$	Constant at 1.649 64
	II	$2.0 \leqslant R \leqslant 30.0$	Tensioned cubic spline fit to the points in Table V, column two
	III	$30.0 \leqslant R$	Constant at − 0.000 078 7
$A\ ^1\Sigma^+$	I	$R \leqslant 2.0$	Constant at − 1.669 62
	II	$2.0 \leqslant R \leqslant 30.0$	Tensioned cubic spline fit to the points in Table V, column three
	III	$30.0 \leqslant R$	Constant at 0.000 275

above the $X\ ^1\Sigma^+$ state dissociation limit and all vibrational wave functions have very small amplitudes. Thus inside $2.0a_0$ the dipole moment is artificially taken as constant. Outside $30.0a_0$ (region III), the dipole moment is essentially zero (see Fig. 2). Only the uppermost vibrational wave function (for $v = 21$) has significant amplitude in this region. The vibrationally averaged dipole moment value for $v = 0, \mu_{v=0}$, occurs at $\sim 3.6a_0$; other μ_v values occur at larger R values. The arrow in the bottom of Fig. 2 marks the location of $\mu_{v=0}$.

The $\mu(R)$ points of Table V are calculated with the electronic wave functions of Olson and Liu.[9] The Olson–Liu calculations use an extended Slater-type function basis set and a very large (6665 configurations) core–valence configuration interaction wave function and produce a $V(R)$ function in excellent agreement with experiment: the depth and minimum of the well are correct ($D_e = 15\,500\ \text{cm}^{-1}$ vs the experimental[1] $D_e = 15\,900 \pm 500\ \text{cm}^{-1}$; $R_e = 3.558a_0$ vs the experimental[10] $R_e = 3.566a_0$), the shape of the well is well characterized [calculated vibrational spacings, $\Delta G_{v+1/2}$ agree within 6 cm^{-1} with the experimental $\Delta G_{v+1/2}$ values of Orth *et al.*[10] ($0 \leqslant v \leqslant 7$) and within 16 cm^{-1} with experimental $\Delta G_{v+1/2}$ values of Giroud and Nedelec[11] ($0 \leqslant v \leqslant 14$); however, as noted above, the B_v values for $v \geqslant 11$ are erratic and thus the Giroud–Nedelec $\Delta G_{v+1/2}$ values may be less certain than the Orth *et al.* values], and the asymptotic behavior is excellent (the calculated electron affinity for H is 0.739 eV vs a measured value of 0.754 eV; the calculated ionization potential for Na is 5.1354 eV vs the experimental value of 5.1426 eV; see Ref. 9 for further details and references). The calculated asymptotes ($3s - 3p$) differ from the atomic lines by 83 cm^{-1} out of 16 968 cm^{-1}.

For comparison purposes, the $\mu(R)$ calculations of Sachs *et al.*[14] are incluced in Fig. 2. Their calculations also use an extensive Slater-type function basis set, but they employ only a 15-configuration multiconfiguration self-consistent field (MCSCF) wave function. Still, the agreement with Olson and Liu's $\mu(R)$ function is quite satisfying.

TABLE V. Theoretical dipole moment functions for $X\ ^1\Sigma^+$ and $A\ ^1\Sigma^+$ states of NaH.

R (a_0)	$X\ ^1\Sigma^+$ state (a.u.)[a,b]	$A\ ^1\Sigma^+$ state (a.u.)[a,b]
2.0	1.649 64	− 1.669 62
2.5	1.969 14	− 1.858 31
3.0	2.227 78	− 1.834 04
3.5	2.474 73	− 1.696 57
4.0	2.708 74	− 1.472 08
4.5	2.910 26	− 1.161 67
5.0	3.048 23	− 0.752 86
5.5	3.080 96	− 0.220 63
6.0	2.959 43	0.469 24
6.5	2.646 27	1.341 58
7.0	2.158 10	2.369 22
7.5	1.593 54	3.444 53
8.0	1.081 18	4.430 77
8.5	0.693 22	5.247 21
9.0	0.431 00	5.881 77
9.5	0.264 19	6.349 59
10.0	0.161 07	6.659 69
10.5	0.098 042	6.801 52
11.0	0.059 643	6.741 25
12.0	0.021 993	5.797 97
13.0	0.007 987	3.736 92
14.0	0.002 754	1.764 75
15.0	0.000 826 2	0.731 14
18.0	− 0.000 236 1	0.057 76
20.0	− 0.000 236 1	0.012 43
30.0	− 0.000 078 7	0.000 275

[a] 1 a.u. = 1 $e\,a_0$ = 2.5418 D.

[b] The last figure is not considered significant, but is included because of its effect on the spline fit to the calculated data.

B. $A\ ^1\Sigma^+$ state of NaH

The dipole moment function for the $A\ ^1\Sigma^+$ state (see Fig. 3) is constructed in a fashion similar to that for the X state: in the physically important region II (from 2.0 to $30.0a_0$), $\mu(R)$ consists of a spline fit to the points given in Table V, while for regions I ($R \leqslant 2.0a_0$) and III ($R \geqslant 30.0a_0$) $\mu(R)$ is artificially taken as constant (see Table IV). The reasons for this constancy outside region II have already been given. In Fig. 3 the location of two vibrationally averaged dipole moments ($\mu_{v=0}$ and $\mu_{v=12}$) are marked with arrows; μ_{12} corresponds to the value where experimental data are first available. Note also, contrary to the situation[3] for the $A\ ^1\Sigma^+$ state in LiH, that μ_v values are positive since $\mu(R) > 0$ for $R > 5.7a_0$.

The points of Table V for the $A\ ^1\Sigma^+$ state are obtained as before with the electronic wave functions of Olson and Liu.[9] The inclusion of diffuse $3s$, $4s$, and $3p$ functions in the basis set provides the ability to correctly characterize the excited A state $V(R)$ and $\mu(R)$ functions, particularly in the "crossover region" (5–$8a_0$) where $\mu(R)$ changes to Na^+H^- polarity.[15] Consistent with the Olson–Liu results for the X state, the $V(R)$ function for the A state is also well characterized: $D_e = 9993\ \text{cm}^{-1}$ at $R_e = 5.992a_0$ vs the experimental[1,10] values $D_e = 10\,137 \pm 500\ \text{cm}^{-1}$ at $R_e = 6.035a_0$; calculated $\Delta G_{v+1/2}$ values agree within 2 cm^{-1} of the experimental $\Delta G_{v+1/2}$ values[10] for $0 \leqslant v \leqslant 19$.

Figure 3 plots the present $\mu(R)$ function and that of Sachs *et al.*[14] To be consistent with the experiments of

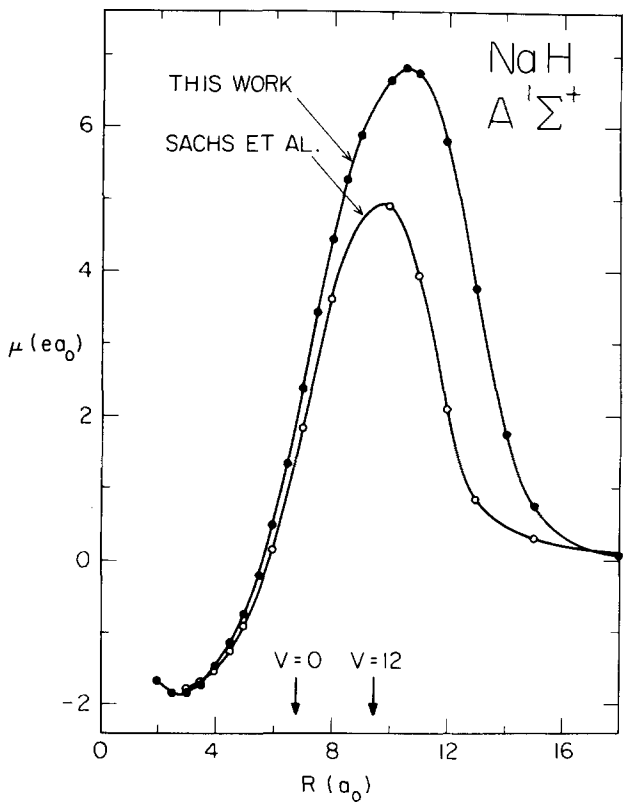

FIG. 3. Dipole moment function $\mu(R)$ (in a.u.) for the $A\,^1\Sigma^+$ state of NaH. The smooth curves through the data are spline fits to the points found in Table V or Sachs *et al.* (Ref. 14). The arrows indicate the R locations corresponding to the vibrationally averaged dipole moments $\mu_{v=0}$ and $\mu_{v=12}(J=0)$.

et al.,[16] the maximum of the Sachs *et al.* theoretical $\mu(R)$ function should be larger in magnitude and shifted to a larger internuclear distance. The comparison presented in Fig. 3 reinforces that conclusion. Although the Sachs *et al.* calculations reasonably determine the depth and shape of the well near R_e, the ability to properly represent both ionic and covalent character over a wide range of R values seems a necessary condition for an accurate $\mu(R)$ function (see Ref. 3 for a similar conclusion in the case of LiH). The large configuration interaction wave function of Olson and Liu[9] has sufficient ionic and neutral configurations ("configuration state functions") to yield a noticeably improved $\mu(R)$ function.

IV. RESULTS AND DISCUSSION

A. Calculation of vibrational-rotational matrix elements

There are four basic kinds of spectroscopic intensity measurements, depending upon whether absorption or emission is involved, and whether photon or energy flux is detected. An excellent discussion of the different quantities with conversion factors is given by Wiese, Smith, and Glennon.[17] In this work we are concerned with evaluating the dipole moment matrix elements

$$\mu_{v',J';v'',J''} = \int_0^\infty \psi_{v',J'}(R)\,\mu(R)\,\psi_{v'',J''}(R)\,dR,$$

where $\psi_{v',J'}$ and $\psi_{v'',J''}$ are the upper and lower normalized vibrational-rotational radial wave functions, respectively. When $v = v' = v''$ and $J = J' = J''$, we have the dipole moment expectation value in the v,J level ($\mu_{v,J}$) which is directly comparable to the experimental value.

We also compute the Einstein A coefficients ($A_{v',J';v'',J''}$) which are proportional to the square of the dipole moment matrix elements ($\mu_{v',J';v'',J''}$) and the cube of the transition frequency

$$[\nu_{v',J';v'',J''} = h^{-1}(E_{v',J'} - E_{v'',J''})].$$

The total Einstein $A_{v',J'}$ coefficient arising from all bound $\rightarrow$bound transitions in either the $X\,^1\Sigma^+ \rightarrow X\,^1\Sigma^+$ or $A\,^1\Sigma^+ \rightarrow A\,^1\Sigma^+$ band systems may be obtained from the expression

$$A_{v',J'} = \left[\frac{1}{2J'+1}\right]\left[(J')\sum_{v''} A_{v',J';v'',J'-1} + (J'+1)\sum_{v''} A_{v',J';v'',J'+1}\right].$$

The reciprocals of the $A_{v',J'}$ values are the radiative lifetimes $\tau_{v',J'}$ within the $X\,^1\Sigma^+$ or $A\,^1\Sigma^+$ manifolds.

The calculations have been carried out using an extensively modified version[18] of the diatomic intensity factor program of Zare and co-workers,[19] based on the Numerov–Cooley numerical solution of the radial Schrödinger equation. The calculations were carried out with a 0.005 Å grid from 1.0 to 13.0 Å ($24.6a_0$) and found to be converged both with respect to the grid spacing and to the inner and outer integration limits.

B. Dipole moment expectation values

In Table VI we record the dipole moment expectation values for both $X\,^1\Sigma^+$ and $A\,^1\Sigma^+$ states. The numbers in Table VI are for $J = 0$, i.e., $\mu_{v,0}$, while the expectation values plotted in Fig. 4 are for $J = 1$ to allow the addition of experimental values to the plot. The differences between $\mu_{v,J=1}$ and $\mu_{v,J=0}$ values are so small that a plot of $\mu_{v,0}$ would appear identical to that of $\mu_{v,1}$ shown in Fig. 4. Except for the values for the three highest vibrational levels in each state, these differences are $\leqslant 0.0022$ a.u. Table VI is a comparison of selected calculated expectation values and experimental values for both states. The comparison with experiment with our $\mu(R)$ function is very good, within experimental uncertainty (see Table VII and Fig. 4). The results using the Sachs *et al.*[14] $\mu(R)$ function for the $X\,^1\Sigma^+$ state agree within 0.1 a.u. of our results (both are within the uncertainty of the one available experimental[20] value $\mu_{v=0,J=1}$).

The results using the Sachs *et al.* $\mu(R)$ function for the $A\,^1\Sigma^+$ state differ significantly from our results and the measured values of Brieger *et al.*[16] Clearly, the Sachs *et al.* $\mu(R)$ function for the A state is not nearly as good as that for the X state. In addition, the values reported in Sachs *et al.*[21] using their $\mu(R)$ function and their theoretical potential curve (numbers in parentheses, Table VII), when compared with values using the experimentally based potential curve, show that an accurate $V(R)$ function is also important for calculating accurate $\mu_{v,J}$ values.

TABLE VI. Expectation values μ_v of the dipole moment function and lifetimes τ_v for all vibrational levels of the $X\,^1\Sigma^+$ and $A\,^1\Sigma^+$ states of NaH.

Vibrational level v	$X\,^1\Sigma^+$ state		$A\,^1\Sigma^+$ state	
	μ_v (a.u.)	τ_v (ms)	μ_v (a.u.)	τ_v (ms)
0	2.5280	∞	0.5589	∞
1	2.5697	28.74	0.6544	29.78
2	2.6100	15.42	0.7801	13.43
3	2.6481	11.03	0.9284	8.350
4	2.6836	8.877	1.0878	5.989
5	2.7157	7.603	1.2561	4.659
6	2.7432	6.761	1.4287	3.821
7	2.7652	6.155	1.6036	3.251
8	2.7801	5.677	1.7801	2.843
9	2.7859	5.264	1.9564	2.539
10	2.7804	4.888	2.1310	2.304
11	2.7608	4.520	2.3031	2.118
12	2.7243	4.159	2.4722	1.968
13	2.6679	3.817	2.6364	1.844
14	2.5862	3.533	2.7947	1.740
15	2.4695	3.350	2.9475	1.652
16	2.3062	3.308	3.0939	1.576
17	2.0879	3.436	3.2337	1.510
18	1.8094	3.794	3.3677	1.454
19	1.4515	4.600	3.4953	1.405
20	0.9287	7.260	3.6138	1.364
21	0.3723	18.11	3.7165	1.325
22			3.7982	1.287
23			3.8627	1.253
24			3.9180	1.230
25			3.9516	1.215
26			3.9379	1.202
27			3.8673	1.204
28			3.7238	1.219
29			3.4840	1.273
30			3.0914	1.411
31			2.4410	1.788
32			1.4901	2.919

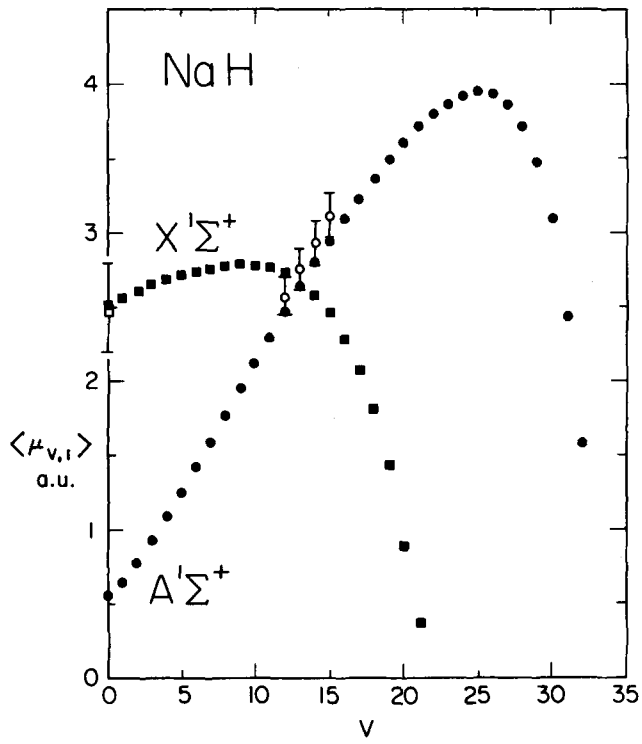

FIG. 4. The solid squares and circles are expectation values of the dipole moment μ_v (in a.u.) for $v = 0$–21 levels of the $X\,^1\Sigma^+$ state and $v = 0$–32 levels of the $A\,^1\Sigma^+$ state of NaH (all $J = 1$), respectively. The open square and circles are experimental values for the $X\,^1\Sigma^+$ state (Ref. 20) (for $v = 0, J = 1$) and the $A\,^1\Sigma^+$ state (Ref. 16) ($v = 12$–$15, J = 1$), respectively, including the range of uncertainty.

C. Dipole moment matrix elements, Einstein *A* coefficients, and lifetimes

The dipole moment function matrix elements and Einstein A coefficients (spontaneous photon emission intensities in s^{-1}) as defined above are given in Table VIII for all vibra-

TABLE VII. Comparison of dipole moment expectation values $\mu_{v,J}$ (in a.u.) for $X\,^1\Sigma^+$ and $A\,^1\Sigma^+$ states of NaH. Our results and those of Sachs *et al.* (Ref. 14) differ in the $\mu(R)$ functions; both calculations use the same experimentally based potentials reported here.

	$J = 0$		$J = 1$		
v	This work	Sachs *et al.* $\mu(R)$	This work	Sachs *et al.* $\mu(R)$	Experiment
$X\,^1\Sigma^+$ state					
0	2.5280	2.6477(2.674)[a]	2.5282	2.6480	2.5 ± 0.3[b]
5	2.7157	2.8298(2.852)[a]	2.7159	2.8300	
10	2.7804	2.9060(2.928)[a]	2.7804	2.9069	
$A\,^1\Sigma^+$ state					
0	0.5589	0.2547(0.189)[a]	0.5611	0.2566	
5	1.2561	0.8555(0.760)[a]	1.2577	0.8569	
10	2.1310	1.5859(1.453)[a]	2.1324	1.5870	
12	2.4722	1.8481	2.4735	1.8491	2.59 ± 0.13[c]
13	2.6364	1.9659	2.6376	1.9668	2.76 ± 0.14[c]
14	2.7947	2.0725	2.7959	2.0733	2.94 ± 0.15[c]
15	2.9475	2.1675	2.9486	2.1682	3.12 ± 0.16[c]

[a] Values in parentheses are those reported in Ref. 21 using the Sachs *et al.* (Ref. 14) $\mu(R)$ *and ab initio* $V(R)$ rather than an experimental potential.
[b] Reference 20.
[c] Reference 16.

tional levels v' and v'' of the $X\ ^1\Sigma^+$ state of NaH. As noted in Ref. 1, the $X\ ^1\Sigma^+$ state of NaH bears striking similarity to the $X\ ^1\Sigma^+$ state of LiH. With regard to radiative transition probabilities (as seen from Table VIII), for $v > 9$ both absorption (proportional to $|\mu|^2$) and emission (proportional to $A_{v,J}$) transitions deviate strongly from the harmonic oscillator selection rule ($\Delta v = \pm 1$). This is quite consistent with the results[22] for the vibrational levels of the $X\ ^1\Sigma^+$ state of LiH.

Since spontaneous emission from the $A\ ^1\Sigma^+$ to the $X\ ^1\Sigma^+$ state will predominate over any spontaneous emis-

TABLE VIII. Dipole moment absorption matrix elements $\mu_{v',J'=0;v'',J''=1}$ [e Å units, in upper right including pure rotational transitions on the diagonal] and Einstein A spontaneous emission coefficients $A_{v',J'=0;v'',J''=1}$ (in s^{-1} units, in lower left) for the $X\ ^1\Sigma^+ \rightarrow X\ ^1\Sigma^+$ bands in NaH. A coefficients are in exponential notation, e.g., 3.485(1) = 34.85.

	$v''(J''=0)$							
$v'(J'=0)$	0	1	2	3	4	5	6	7
0	1.337 804	0.059 682	− 0.007 263	0.000 914	− 0.000 184	0.000 044	− 0.000 013	0.000 007
1	3.479(1)	1.359 904	0.083 189	− 0.013 003	0.001 848	− 0.000 420	0.000 118	− 0.000 036
2	4.083(0)	6.076(1)	1.381 234	0.099 866	− 0.019 058	0.002 957	− 0.000 727	0.000 234
3	2.097(− 1)	1.180(1)	7.866(1)	1.401 384	0.112 292	− 0.025 599	0.004 291	− 0.001 121
4	1.903(− 2)	7.723(− 1)	2.283(1)	8.903(1)	1.420 170	0.121 228	− 0.032 703	0.005 848
5	1.981(− 3)	8.971(− 2)	1.780(0)	3.701(1)	9.265(1)	1.437 123	0.126 929	− 0.040 432
6	2.662(− 4)	1.314(− 2)	2.414(− 1)	3.367(0)	5.412(1)	9.016(1)	1.451 685	0.129 281
7	1.233(− 4)	1.961(− 3)	4.599(− 2)	5.139(− 1)	5.599(0)	7.380(1)	8.250(1)	1.463 316
8	1.146(− 4)	4.848(− 4)	1.024(− 2)	1.135(− 1)	9.255(− 1)	8.619(0)	9.580(1)	7.068(1)
9	7.414(− 5)	4.209(− 4)	2.918(− 3)	2.959(− 2)	2.308(− 1)	1.521(0)	1.259(1)	1.196(2)
10	2.742(− 5)	5.753(− 4)	1.395(− 3)	9.612(− 3)	7.085(− 2)	4.122(− 1)	2.332(0)	1.770(1)
11	8.941(− 6)	5.938(− 4)	1.198(− 3)	4.730(− 3)	2.580(− 2)	1.403(− 1)	6.769(− 1)	3.366(0)
12	9.154(− 6)	4.119(− 4)	1.358(− 3)	3.573(− 3)	1.209(− 2)	5.763(− 2)	2.421(− 1)	1.038(0)
13	2.185(− 5)	2.053(− 4)	1.492(− 3)	3.316(− 3)	8.108(− 3)	2.767(− 2)	1.050(− 1)	3.891(− 1)
14	4.154(− 5)	9.157(− 5)	1.370(− 3)	3.185(− 3)	7.024(− 3)	1.601(− 2)	5.369(− 2)	1.710(− 1)
15	5.156(− 5)	5.636(− 5)	1.019(− 3)	2.951(− 3)	6.404(− 3)	1.165(− 2)	3.097(− 2)	8.796(− 2)
16	4.388(− 5)	5.829(− 5)	6.345(− 4)	2.544(− 3)	5.528(− 3)	9.917(− 3)	1.992(− 2)	5.163(− 2)
17	2.732(− 5)	7.299(− 5)	3.577(− 4)	2.003(− 3)	4.474(− 3)	8.704(− 3)	1.432(− 2)	3.315(− 2)
18	1.296(− 5)	8.246(− 5)	1.988(− 4)	1.430(− 3)	3.432(− 3)	7.244(− 3)	1.109(− 2)	2.229(− 2)
19	4.709(− 6)	7.562(− 5)	1.133(− 4)	9.160(− 4)	2.447(− 3)	5.439(− 3)	8.475(− 3)	1.491(− 2)
20	1.246(− 6)	4.868(− 5)	5.748(− 5)	4.664(− 4)	1.387(− 3)	3.164(− 3)	5.165(− 3)	8.306(− 3)
21	2.696(− 7)	1.918(− 5)	2.091(− 5)	1.647(− 4)	5.222(− 4)	1.203(− 3)	2.026(− 3)	3.134(− 3)

	$v''(J''=0)$						
$v'(J'=0)$	8	9	10	11	12	13	14
0	− 0.000 006	0.000 004	− 0.000 002	0.000 001	− 0.000 001	0.000 001	− 0.000 002
1	0.000 015	− 0.000 011	0.000 011	− 0.000 010	0.000 007	− 0.000 005	0.000 003
2	− 0.000 086	0.000 038	− 0.000 022	0.000 017	− 0.000 016	0.000 015	− 0.000 013
3	0.000 388	− 0.000155	0.000 072	− 0.000 043	0.000 032	− 0.000 027	0.000 024
4	− 0.001591	0.000 586	− 0.000 254	0.000 125	− 0.000 072	0.000 051	− 0.000 042
5	0.007 684	− 0.002 162	0.000 832	− 0.000 381	0.000 200	− 0.000 117	0.000 077
6	− 0.048 892	0.009 862	− 0.002 847	0.001 136	− 0.000 534	0.000 289	− 0.000 175
7	0.127 962	− 0.058 140	0.012 458	− 0.003 649	0.001 503	− 0.000 726	0.000 395
8	1.471 164	0.122 517	− 0.068 205	0.015 608	− 0.004 596	0.001 936	− 0.000 957
9	5.598(1)	1.474 224	0.112 328	− 0.079 061	0.019 471	− 0.005 725	0.002 445
10	1.441(2)	3.995(1)	1.471 290	0.096 671	− 0.090 547	0.024 219	− 0.007 082
11	2.429(1)	1.683(2)	2.443(1)	1.460 904	0.074 875	− 0.102 226	0.030 172
12	4.661(0)	3.279(1)	1.902(2)	1.145(1)	1.441 563	0.046 320	− 0.113 286
13	1.495(0)	6.263(0)	4.367(1)	2.072(2)	2.844(0)	1.411 696	0.009 680
14	5.843(− 1)	2.054(0)	8.215(0)	5.764(1)	2.143(2)	1.967(− 2)	1.368 399
15	2.625(− 1)	8.278(− 1)	2.727(0)	1.073(1)	7.684(1)	2.028(2)	4.182(0)
16	1.343(− 1)	3.790(− 1)	1.149(0)	3.513(0)	1.460(1)	1.034(2)	1.643(2)
17	7.682(− 2)	1.985(− 1)	5.320(− 1)	1.576(0)	4.450(0)	2.252(1)	1.320(2)
18	4.796(− 2)	1.137(− 1)	2.749(− 1)	7.602(− 1)	2.097(0)	5.922(0)	3.932(1)
19	3.078(− 2)	6.667(− 2)	1.526(− 1)	3.829(− 1)	1.059(0)	2.525(0)	1.014(1)
20	1.672(− 2)	3.370(− 2)	7.533(− 2)	1.748(− 1)	4.665(− 1)	1.154(0)	3.018(0)
21	6.216(− 3)	1.209(− 2)	2.677(− 2)	5.972(− 2)	1.549(− 1)	3.966(− 1)	8.849(− 1)

TABLE VIII. (*Continued*)

	$v''(J''=1)$						
$v'(J'=0)$	15	16	17	18	19	20	21
0	0.000 002	− 0.000 002	0.000 001	− 0.000 001	0.000 000	0.000 000	0.000 000
1	− 0.000 002	0.000 002	− 0.000 002	0.000 002	− 0.000 002	0.000 002	− 0.000 001
2	0.000 010	− 0.000 008	0.000 005	− 0.000 004	0.000 003	− 0.000 002	0.000 001
3	− 0.000 021	0.000 018	− 0.000 015	0.000 012	− 0.000 009	0.000 006	− 0.000 004
4	0.000 036	− 0.000 030	0.000 025	− 0.000 021	0.000 017	− 0.000 012	0.000 007
5	− 0.000 058	0.000 048	− 0.000 041	0.000 035	− 0.000 029	0.000 021	− 0.000 013
6	0.000 115	− 0.000 082	0.000 063	− 0.000 051	0.000 042	− 0.000 032	0.000 019
7	− 0.000 241	0.000 161	− 0.000 116	0.000 087	− 0.000 066	0.000 047	− 0.000 028
8	0.000 530	− 0.000 324	0.000 216	− 0.000 154	0.000 114	− 0.000 080	0.000 048
9	− 0.001 234	0.000 695	− 0.000 435	0.000 293	− 0.000 205	0.000 137	− 0.000 080
10	0.003 061	− 0.001 593	0.000 912	− 0.000 573	0.000 385	− 0.000 253	0.000 146
11	− 0.008 821	0.003 823	− 0.002 077	0.001 229	− 0.000 773	0.000 483	− 0.000 273
12	0.038 231	− 0.011 398	0.004 823	− 0.002 724	0.001 677	− 0.001 013	0.000 560
13	− 0.122 208	0.049 717	− 0.016 066	0.006 395	− 0.003 503	0.002 116	− 0.001 179
14	− 0.037 218	− 0.125 552	0.064 934	− 0.024 920	0.009 989	− 0.004 713	0.002 395
15	1.306 592	− 0.095 643	− 0.117 753	0.080 955	− 0.039 132	0.017 800	− 0.008 336
16	1.476(1)	1.220 006	− 0.163 873	− 0.091 573	0.089 238	− 0.052 577	0.026 983
17	1.024(2)	2.724(1)	1.104 408	− 0.234 657	− 0.039 132	0.069 620	− 0.045 281
18	1.420(2)	3.903(1)	3.398(1)	0.956 879	− 0.294 208	0.043 845	0.006 931
19	6.415(1)	1.072(2)	3.087(0)	2.858(1)	0.767 251	− 0.309 421	0.119 933
20	1.973(1)	6.526(1)	3.228(1)	4.165(0)	1.135(1)	0.490 071	− 0.226 695
21	5.164(0)	2.191(1)	1.985(1)	1.181(− 2)	5.959(0)	7.810(− 1)	0.195 436

sion within the $A\ ^1\Sigma^+$ state, no Einstein coefficients for the A state are presented. However, spontaneous radiative lifetimes for both X–X and A–A radiative transitions are presented in Table VI. The trend in lifetimes with increasing v parallels that trend in X[22] and A[3] states of LiH. However, based on comparison with the A state[3] of LiH, we expect the τ_v for the very last long-range level in the A state of NaH to increase to a value of 10–100 ms. This would happen if another level corresponding to $v = 33$ occurred with a very small binding energy. Based on earlier studies[3,4,22] on long-range levels in LiH and limited preliminary calculations on NaH, we predict the existence of another level in the A state of NaH within $\ll 1\ \text{cm}^{-1}$ of the dissociation limit. Full characterization of that level will occur at a later time.

Finally, we are aware of only one other $\mu(R)$ calculation, that of Meyer and Rosmus[23] who report a linear $\mu(R)$ function for the *limited* region of 3–5a_0 for the $X\ ^1\Sigma^+$ state only. Their linear $\mu(R)$ function would overlay our curve from 3–4a_0, but fails to bend over in the 4–5a_0 region; see Fig. 2.

V. CONCLUSIONS

In this work we report for both $X\ ^1\Sigma^+$ and $A\ ^1\Sigma^+$ states of NaH (1) new hybrid potential energy curves $V(R)$ for all R and (2) new dipole moment functions $\mu(R)$ that we consider to be improved over previous theoretical work. The $\mu(R)$ functions are calculated with a very large configuration-interaction wave function and an extended Slater basis set which includes diffuse 3s, 4s, and 3p functions. Expectation values of the dipole moment μ_v for all 22 vibrational levels of the X state and for 33 levels of the A state are reported. Values with a nonzero rotational quantum number are compared with measured and other theoretical values. The good agreement with experiment supports our contention that these $\mu(R)$ functions are of high quality.

Both potential curves are constructed from RKR experimental curves in the vicinity of the minimum of the well and from scaled *ab initio* $V(R)$ functions in the intermediate to long-range internuclear distance region; proper asymptotic behavior is obtained with $-C_n/R^n$ expansions near the dissociation limit. In the case of the $X\ ^1\Sigma^+$ state, a new and improved RKR curve is reported.

Dipole moment absorption matrix elements and Einstein A coefficients for spontaneous emission within the $X\ ^1\Sigma^+$ state are presented. Spontaneous radiative lifetimes for both X and A states are reported; there appear to be no measurements of these lifetimes. Similarities with earlier calculations on the $X\ ^1\Sigma^+$ state[22] and $A\ ^1\Sigma^+$ state[3] of ^{7}LiH are noted. Based on such a comparison, we predict that in the $A\ ^1\Sigma^+$ state of NaH there should be another vibrational level ($v' = 33$) very close to the dissociation limit.

ACKNOWLEDGMENTS

Part of this work was done by one of us (WTZ) while in residence the summer of 1981 as a NASA/ASEE Faculty Fellow at NASA Ames Research Center, Moffett Field, California. We would like to gratefully acknowledge this support and the assistance of the Computational Chemistry Group at Ames, particularly that of Stephen Langhoff and Harry Partridge. Work at Iowa was supported by the National Science Foundation. We also wish to thank Professor Joel Tellinghuisen for his RKR program[24] used in this work.

[1]S. C. Yang and W. C. Stwalley, ACS Symp. Ser. **179**, 241 (1982).
[2]W. C. Stwalley and S. C. Yang, Proceedings of the 38th Symposium on Molecular Spectroscopy, Columbus, Ohio, 1983; J. Phys. Chem. Ref. Data (submitted).
[3]H. Partridge, S. R. Langhoff, W. C. Stwalley, and W. T. Zemke, J. Chem. Phys. **75**, 2299 (1981).
[4]W. C. Stwalley, W. T. Zemke, K. R. Way, K. C. Li, and T. R. Proctor, J. Chem. Phys. **66**, 5412 (1977); **67**, 4785(E) (1977).
[5]T. R. Proctor and W. C. Stwalley, J. Chem. Phys. **66**, 2063 (1977).
[6]R. J. LeRoy, in *Molecular Spectroscopy 1*, edited by R. F. Barrow, D. A. Long, and D. J. Millin (Chemical Society, London, 1973), p. 113.
[7]The breakdown occurs inside $R_c = 2[\langle r^2\rangle_{Na}^{1/2} + \langle r^2\rangle_H^{1/2}]$. Since $\langle r^2\rangle$ for hydrogenic atoms equals $(n^*)^2/2[5(n^*)^2 + 1 - 3l(l+1)]$, where n^* is the effective principal quantum number (see Ref. 8), one readily obtains R_c for these states [as in previous work (Ref. 4) on LiH].
[8]T. R. Proctor and W. C. Stwalley, Mol. Phys. **37**, 1969 (1979).
[9]R. E. Olson and B. Liu, J. Chem. Phys. **73**, 2817 (1980).
[10]F. B. Orth, W. C. Stwalley, S. C. Yang, and Y. K. Hsieh, J. Mol. Spectrosc. **79**, 314 (1980).
[11]M. Giroud and O. Nedelec, J. Chem. Phys. **73**, 4151 (1980).
[12]K. V. L. N. Sastry, E. Herbst, and F. C. DeLucia, J. Chem. Phys. **75**, 4753 (1981).
[13]$C_6(\text{NaH}) = [n^*(\text{Na } 3p)/n^*(\text{Li } 2p)]^4 \cdot C_6(\text{LiH})$ and $C_8(\text{NaH}) = (n^*_{Na}/n^*_{Li})^8 \cdot C_8(\text{LiH})$. See Ref. 4 for information on the C_6 and C_8 coefficients for the $A\ ^1\Sigma^+$ state of LiH.
[14]E. S. Sachs, J. Hinze, and N. H. Sabelli, J. Chem. Phys. **62**, 3367 (1975).
[15]Further discussion on this type of behavior in the anomalous $A\ ^1\Sigma^+$ state $V(R)$ and $\mu(R)$ functions for LiH can be found in Ref. 3. The behavior of the $A\ ^1\Sigma^+$ state in NaH is similar to that in LiH. Reference 1 analyzes ionic-covalent interactions and calculates avoided crossing distances (Landau–Zener model) and coupling matrix elements between $A\ ^1\Sigma^+$ and $X\ ^1\Sigma^+$ states in all the alkali hydrides.
[16]M. Brieger, A. Hese, A. Renn, and A. Sodeik, Chem. Phys. Lett. **78**, 153 (1981).
[17]W. L. Wiese, M. W. Smith, and B. M. Glennon, *Atomic Transition Probabilities, Volume 1, Hydrogen Through Neon*, Nat. Bur. Stand. (U. S. GPO, Washington, D.C., 1966).
[18]W. T. Zemke and W. C. Stwalley, Quantum Chemistry Program Exchange Bulletin (in press).
[19]R. N. Zare, J. Chem. Phys. **40**, 1934 (1964).
[20]P. J. Dagdigian, J. Chem. Phys. **71**, 2328 (1979).
[21]E. S. Sachs, J. Hinze, and N. H. Sabelli, J. Chem. Phys. **62**, 3367 (1975).
[22]W. T. Zemke and W. C. Stwalley, J. Chem. Phys. **73**, 5584 (1980).
[23]W. Meyer and P. Rosmus, J. Chem. Phys. **63**, 2356 (1975).
[24]J. Tellinghuisen, Comput. Phys. Commun. **6**, 221 (1974).